

# On the c-axis optical reflectivity of layered cuprate superconductors

S. Das Sarma and E. H. Hwang

*Center for Superconductivity Research, Department of Physics*

*University of Maryland, College Park, Maryland 20742-4111*

(May 10, 2018)

## Abstract

Using a conventional BCS – Fermi liquid model we calculate the c-axis optical reflectivity of the layered high temperature cuprate superconductors by obtaining the finite temperature dynamical dielectric function in a microscopic self-consistent gauge invariant formalism. We get good semi-quantitative agreement with all the existing experimental data by using the measured normal state *dc* resistivities as the input parameters in obtaining the c-axis hopping amplitude and the normal state level broadening in our microscopic calculation.

PACS Number : 74.20.-z;74.72.-h;71.45.Gm;74.25.Gz

The c-axis charge dynamics of high-temperature layered cuprate superconductors is unusual and interesting, and has therefore attracted a great deal of well-deserved attention. In this Letter we present a microscopic theoretical calculation for the c-axis optical reflectivity of the cuprates, concentrating on the optimum doping (normally corresponding to the highest critical temperature  $T_c$ ) single layer (eg. LSCO, Tl-2201) cuprate systems which have only one CuO layer per unit cell. An impressive series [1–3] of c-axis optical reflectivity measurements by Uchida and co-workers on single-crystal  $La_{1-x}Sr_xCuO_4$  (LSCO) systems shows the following salient features in the frequency dependence of the electronic reflectivity: (1) For temperatures  $T > T_c$ , *i.e.*, in the normal phases, the c-axis optical reflectivity is essentially structureless down to  $20\text{ cm}^{-1}$  (the lowest frequency studied in ref. [1]), and the data resemble that of an ionic insulator; (2) in the superconducting phase, for  $T < T_c$ , the reflectivity develops a well-defined sharp plasma edge with the effective plasma frequency,  $\omega_{pl}$  (defined as the frequency where the real part of the dielectric function goes through a zero,  $\text{Re}\epsilon(\omega_{pl}) = 0$ ), being below the superconducting energy gap  $\Delta$  (in fact,  $\omega_{pl} \sim 50\text{ cm}^{-1}$  in optimally doped LSCO) – thus the superconducting state exhibits a classic “metallic” optical reflectivity behavior in contrast to the normal state “insulating” behavior; (3) the very low c-axis plasma frequency (below the energy gap) associated with the observed reflectivity plasma edge corresponds to a carrier mass substantially larger than the c-axis optical mass obtained in standard band structure calculations, *i.e.*, the experimental  $\omega_{pl}$  is much smaller, by more than an order of magnitude, than the corresponding local-density-approximation (LDA) band structure calculated value; (4) the superconducting state plasma edge shows a characteristic temperature dependence, becoming weaker (and  $\omega_{pl}(T)$  shifting to lower frequency with increasing temperature) as  $T$  approaches  $T_c$  from below; (5) the plasma edge shows a strong doping dependence. It has been emphasized that these anomalies, in particular, items (1)-(3) above, are very difficult to understand on the basis of the standard Fermi liquid BCS-type generic theories of high temperature superconductors.

In the theoretical work presented here we obtain the c-axis reflectivity of the layered cuprate materials by calculating the appropriate long wavelength dynamical dielectric func-

tion  $\epsilon(\omega)$  of the system. In calculating the long wavelength frequency dependent dielectric function we use the Nambu-Gorkov formalism [4] and carry out a fully gauge invariant self-consistent finite temperature linear response calculation [5] including “impurity scattering” induced level broadening effects in the theory [6]. Our theory, therefore, corresponds to the one [5] developed by Fertig and Das Sarma for anisotropic layered superconducting systems except for three important generalizations beyond ref. [5]: (1) we use a finite temperature formalism in contrast to the  $T = 0$  case studied in ref. [5], (2) we use the d-wave order parameter symmetry for the superconducting ground state in our response calculation [7] in contrast to the  $s$ -wave model used in ref. [5] (this turns out to be unimportant in understanding reflectivity measurements), and (3) we include level broadening effects in our microscopic calculation in contrast to ref. [5] which neglected disorder. We point out that the  $d$ -wave symmetry makes negligible difference [7] with respect to the  $s$ -wave symmetry in our long wavelength dielectric response calculation (there are substantial differences [7] at large wave vectors, which are not of any significance to optical reflectivity measurements). Inclusion of level broadening in the dynamical dielectric function is, however, crucial in understanding the c-axis reflectivity measurements – in particular, strong disorder scattering in these systems, as reflected in their anomalously high c-axis  $dc$  resistivities for  $T > T_c$ , gives rise to an overdamped plasmon in the normal state, completely suppressing any normal state metallic plasma edge for  $T > T_c$ . A plasma edge in the superconducting state corresponding to the c-axis Anderson-Bogoliubov plasma mode [5,7] is, however, preserved because single particle level broadening does not affect the condensed carriers in the superconducting state.

We assume [5] a simple single tight binding band (of bandwidth  $2t_c$ ) along the c-axis and take the single-particle energy dispersion to be  $E(k, k_z) = \hbar^2 k^2 / 2m - t_c \cos(k_z d)$ , where  $k \equiv |\mathbf{k}_{ab}|$  is the wave vector in the  $ab$  plane (with  $m$  as the planar effective mass for charge dynamics in the  $ab$  plane),  $d$  is the c-axis layer separation, and  $k_z$  the wave vector along the c-axis. Following refs. [5] and [7] we carry out a self-consistent (and gauge invariant) linear response calculation for the dynamical dielectric function  $\epsilon(\omega)$  treating the long range Coulomb interaction (in the highly anisotropic layered system) in the random phase approx-

imation (“bubble” diagrams) and the BCS-like short-range pairing interaction in the ladder approximation (which is a conserving approximation because the BCS self-energy producing the superconductivity is a Hartree-Fock single-loop self-energy). We include level broadening effects both in the single-particle Green’s function and in the vertex correction through the ladder impurity diagrams [6]. Assuming the impurity scattering to be short-ranged and isotropic, we can parameterize the disorder strength by a single level broadening parameter (*i.e.*, an imaginary part of the self-energy)  $\gamma$  where  $\tau = (2\gamma)^{-1}$ , with  $\hbar = 1$  throughout, is the transport relaxation time for the c-axis normal transport properties. Thus in principle, the normal state c-axis resistivity  $\rho_c$  of the system defined  $\gamma$  within our model. The calculated microscopic  $\epsilon(\omega)$  therefore depends on  $\gamma$ ,  $T$ ,  $\Delta$  and  $T_c$  (which are determined [5,7] by the strength of the pairing interaction in our BCS model) as well as on the effective single-particle parameters  $m$  and  $t_c$ . The results depend also on a number of obvious parameters such as the two-dimensional carrier density  $n_{2D}$  (which determines the density of states), the layer separation  $d$  in the c-direction, and the effective background dielectric constant  $\kappa$ . Our philosophy at this stage is to treat  $\gamma$  and  $t_c$ , the two most contentious parameters in our theory, as unknown parameters, and take the other parameters from the best available experimental (and where appropriate, from band structure) results. We note that the details of the pairing interaction or the impurity potential do not affect our reflectivity results in any qualitative way.

In Fig. 1 we show our calculated c-axis optical reflectivity to be compared directly with the experimental results of Tamasaku *et al.* [1]. We have use parameters corresponding to LSCO except for  $t_c$  and  $\gamma$  which are varied to produce different curves in Fig. 1. Our calculated results look *very similar* to the experimental observations (see, for example, Fig. 1 in ref. [1]), and in fact our theory agrees with the measurements *quantitatively* if we treat  $t_c$  and  $\gamma$  as phenomenological parameters and choose  $t_c \approx 0.1\Delta - 0.3\Delta$  and  $\gamma \geq \Delta$ . Typically we find the plasma edge  $\omega_{pl} \approx 2t_c - 4t_c$  in the superconducting state, and provided  $\gamma \geq \Delta$  no plasma edge shows up in the normal state with the normal state reflectivity remaining essentially constant around 0.5 (exactly as in the experimental results of ref. [1]) down

to rather low frequencies ( $\omega \leq 0.1\Delta$ ). We predict that if the normal state reflectivity measurement is pushed down to rather low frequencies ( $\sim 10\text{cm}^{-1}$  or below), one would see a rise in the reflectivity as it would increase to unity to be consistent with there being a finite (albeit very low) *dc* conductivity along the c-axis.

It is clear from the results shown in Fig. 1 that to get agreement with the experimental measurements [1–3] within our model one must have a very low (high) value of the c-axis hopping amplitude  $t_c$  (level broadening parameter  $\gamma$ ). In particular, our theory gives  $\omega_{pl} \sim 2t_c$  in the superconducting state, which constraints  $t_c$  to be in the range of 20 - 30  $\text{cm}^{-1}$  in LSCO for the theory to be quantitatively consistent with the experimental measurement in ref. [1] which finds a sharp reflectivity plasma edge in the 30 - 60  $\text{cm}^{-1}$ . The other striking experimental anomaly [1] of the nonexistence of any reflectivity plasma edge in the normal state is “explained” in our theory by having a large damping or broadening term  $\gamma (\geq \Delta)$  which enters our microscopic impurity scattering diagrams in the dynamical polarizability function. We have so far treated  $t_c$  and  $\gamma$  as phenomenological parameters, and the crucial issue therefore is to justify (or, at least provide a rationale for) having such small (high) values of  $t_c$  ( $\gamma$ ) in layered high temperature superconducting systems. This, in fact, was the basis of the trenchant analysis of the experimental results [1–3] carried out by Anderson [8], which led him to conclude [8] that a standard Fermi liquid-BCS type analysis (exactly of the type we carry out in this work) is incapable of explaining the experimental c-axis reflectivity data.

In this work we treat  $t_c$  and  $\gamma$  as phenomenological parameters to be fixed by *normal state dc* transport properties of the systems. We use the *measured* values of normal state  $\rho_c$  and  $\rho_{ab}$  at  $T \geq T_c$  to fix  $t_c$  and  $\gamma$  within the standard Fermi liquid picture. The hopping amplitude  $t_c$  is then given simply by the formula

$$t_c = \left( \frac{\pi n_{2D}}{2d^2 m^2} \frac{\rho_{ab}}{\rho_c} \right)^{1/2}. \quad (1)$$

The level broadening  $\gamma$  is given simply by the c-axis *dc* resistivity through the usual relaxation time approximation in the tight binding limit:

$$\gamma = \frac{e^2 n_{2D} dt_c \rho_c}{2} = \frac{e^2}{2m} \sqrt{\pi n_{2D}^3 \rho_c \rho_{ab} / 2}. \quad (2)$$

The simple Drude-Boltzmann-Fermi liquid formulae given by Eqs. (1) and (2) immediately explain why the hopping parameter  $t_c$  (the level broadening parameter  $\gamma$ ) is extremely small (large) – both of these anomalies arise from the anomalously large c-axis resistivity, which is a universal feature for the layered cuprates. We should emphasize two significant aspects of the phenomenological analysis giving as the all-important parameters  $t_c$  and  $\gamma$  (from the normal state  $dc$  resistivities of the system): (1) standard LDA band structure calculations [9] give values of  $t_c$  which are one to two orders of magnitude larger than those given by Eq. (1) for layered cuprates (while the two dimensional electron density and the effective mass in the  $ab$  plane seem to be reasonably, *i.e.*, within a factor of two, well-described by LDA band calculations [9]); (2) our Drude-Fermi liquid phenomenological description characterized by Eqs. (1) and (2) is completely independent of the actual normal state transport mechanism along the c-axis and depends only on the crucial observation that the normal state  $dc$  transport along the c-axis is “metallic” around optimal doping (albeit with an anomalously large imaginary part of the self-energy  $\gamma$ ).

In Table 1 we summarize our results for a number of layered cuprates, giving the values of the parameters  $t_c$  and  $\gamma$  (obtained from experimental  $\rho_c$  and  $\rho_{ab}$  at  $T \geq T_c$ ) used in our calculations to obtain  $\omega_{pl}$  at  $T = 0$ , the long wavelength c-axis Anderson-Bogoliubov plasmon frequency in the superconducting phase. In carrying out our microscopic calculation for the “multilayer” cuprates (*e.g.* YBCO, BISCO), which contain more than one CuO layers per unit cell, we are concentrating here only on the low frequency c-axis plasma properties which arise from the *intercell* hopping, neglecting the mode mixing effects arising from the *intracell* hopping between the CuO layers. This is equivalent to making an effective single layer model for these multilayer cuprates, which should suffice for the c-axis reflectivity properties. From the available experimental results given in Table 1 it is clear that our phenomenological theory, utilizing the normal state  $dc$  resistivities as the input parameters for the microscopic calculation of the dielectric response, gives a good semiquantitative description of the c-

axis optical measurements in cuprate superconductors. Understanding the strong doping dependence of the data in ref. [1] requires a more complicated phenomenological model [10] for  $t_c$  and  $\gamma$  because  $\rho_c$  shows, in general, complex doping dependence.

Finally, we point out that a simple phenomenological Casimir-Gorter two fluid description works remarkably well for this problem. Writing the dynamical dielectric function  $\epsilon(\omega)$  as

$$\epsilon(\omega) = 1 - \frac{\omega_{pn}^2}{\omega^2 + i\omega\gamma} - \frac{\omega_{ps}^2}{\omega^2}, \quad (3)$$

where  $\omega_{pn(s)}$  is the normal (superconducting) fluid c-axis plasma frequency in the tight binding description obtained respectively from the normal (superconducting) carrier density, we can calculate (Fig. 2) the c-axis optical reflectivity. These results shown in Fig. 2 look qualitatively similar to our microscopic results shown in Fig. 1. (The detailed temperature dependences in the two descriptions are somewhat different.) The physical picture that emerges from our work is thus simple: large level broadening due to strong scattering (large  $\gamma$ ) in the normal state associated with “incoherent” transport [10] along the c-axis overdamps the normal state c-axis plasmon preventing the formation of a reflectivity edge and producing fairly structureless normal state reflectivity whereas the superconducting carriers, being unaffected by scattering effects, give rise to a sharp reflectivity edge associated with the well-defined Anderson-Bogoliubov c-axis plasmon which lies in the superconducting gap due to weak interlayer carrier hopping in the layered cuprate systems.

## ACKNOWLEDGMENTS

We thank P. W. Anderson, K. A. Moler, and especially, A. J. Millis for helpful discussions. This work is supported by the US-ONR.

## REFERENCES

- [1] K. Tamasaku, Y Nakamura, and S. Uchida, Phys. Rev. Lett. **69**, 1455 (1992).
- [2] K. Tamasaku, T. Iyo, H. Takagi, and S. Uchida, Phys. Rev. Lett. **72**, 3088 (1992).
- [3] S. Uchida, K. Tamasaku, and S. Tajima, Phys. Rev. B **53**, 14 558 (1996), and references therein.
- [4] Y. Nambu, Phys. Rev. **117**, 648 (1960); R. E. Prange, Phys. Rev. **129**, 2495 (1963).
- [5] H. A. Fertig and S. Das Sarma, Phys. Rev. Lett. **65**, 1482 (1990); Phys. Rev. B **44**, 4480 (1991).
- [6] I. O. Kulik, O. Entin-Wohlman, and R. Orbach, J. Low Temp. Phys. **43**, 591 (1981).
- [7] E. H. Hwang and S. Das Sarma, Phys. Rev. B **52**, R7010 (1995).
- [8] P. W. Anderson, Science **268**, 1154 (1995).
- [9] P. B. Allen, W. E. Pickett, and H. Krakauer, Phys. Rev. B **37**, 7482 (1988); W. E. Pickett, Rev. Mod. Phys. **61**, 433 (1989).
- [10] R. J. Radtke and V. N. Kostur, Can. J. Phys. **75**, 363 (1997); and references therein.
- [11] T. Kimura, *et. al.*, Physica C **192**, 247 (1992).
- [12] T. Manako, *et. al.*, Physica C **185-189**, 1327 (1991).
- [13] J. Schützmann, *et. al.*, Phys. Rev. B **55**, 11 118 (1997); K. A. Moler *et. al.*, preprint (1997).
- [14] K. Takenaka, *et. al.*, Phys. Rev. B **50**, 6534 (1994).
- [15] C. C. Homes, *et. al.*, Phys. Rev. Lett. **71**, 1645 (1993).
- [16] S. Martin, *et. al.*, Appl. Phys. Lett. **54**, 72 (1989).
- [17] H. Shibata and T. Yamada, Phys. Rev. B **54**, 7500 (1996).



## TABLES

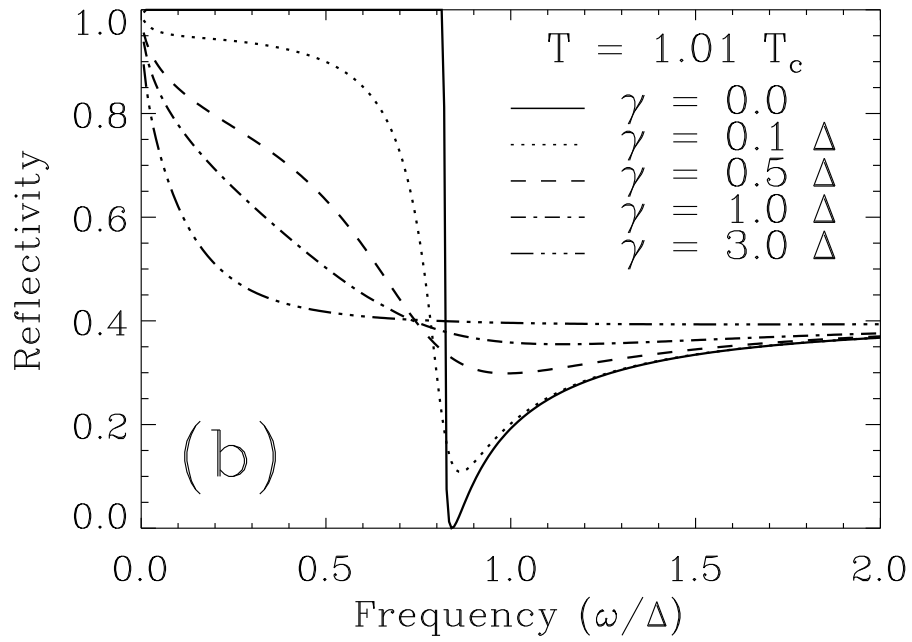
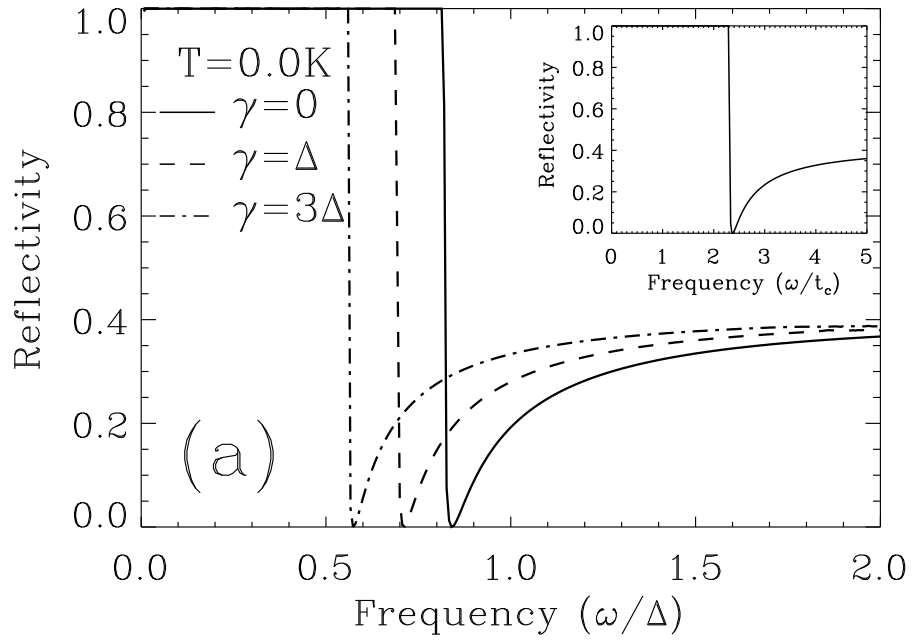
TABLE I. Calculated parameters  $t_c$  and  $\gamma$ , and the corresponding c-axis plasma frequencies ( $\omega_{pl}$ ) for various layered cuprates.

## FIGURES

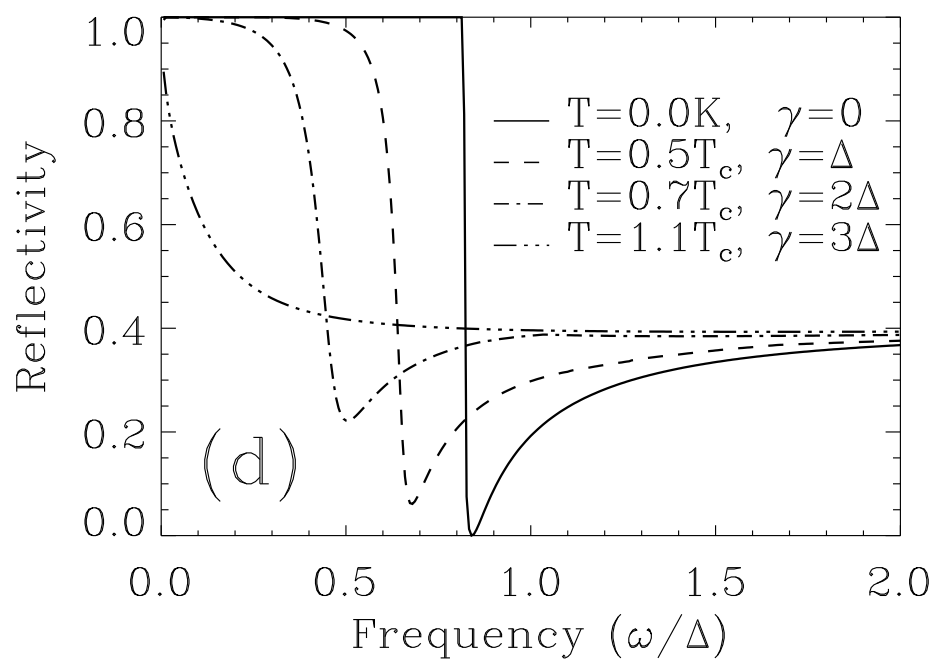
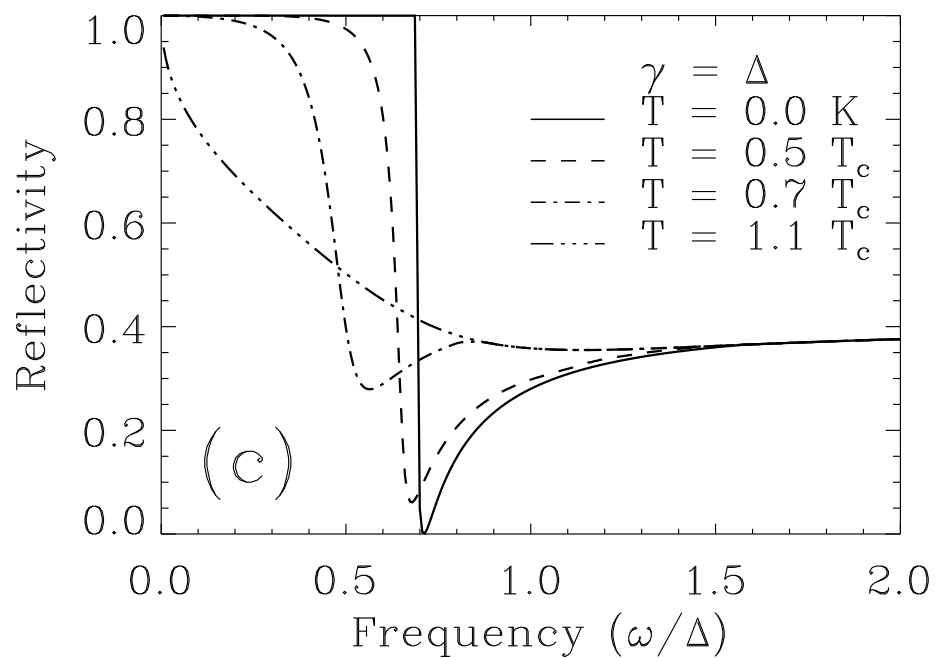
FIG. 1. Reflectivity of LSCO as a function of the frequency (a) for fixed temperature  $T = 0K$  (superconducting state) with various impurity scattering rate  $\gamma$ , (inset shows the reflectivity as a function of the frequency normalized by the hopping parameter  $t_c$  for  $T = 0K$  and  $\gamma = \Delta$ ); (b) for fixed temperature  $T = 1.01T_c$  (normal state) with various  $\gamma$ ; (c) for fixed impurity scattering rate  $\gamma = \Delta$  with different temperatures, and (d) for various  $T$  and  $\gamma$ .

FIG. 2. (a) Reflectivity of  $La_{2-x}Sr_xCuO_4$  ( $x = 0.16$ ) from the two-fluid model for different temperatures  $t = T/T_c$  as a function of the frequency normalized by the hopping amplitude  $t_c$ . (b) The same as in (a) for  $Tl_2Ba_2CuO_6$  ( $T_c = 85K$ ).

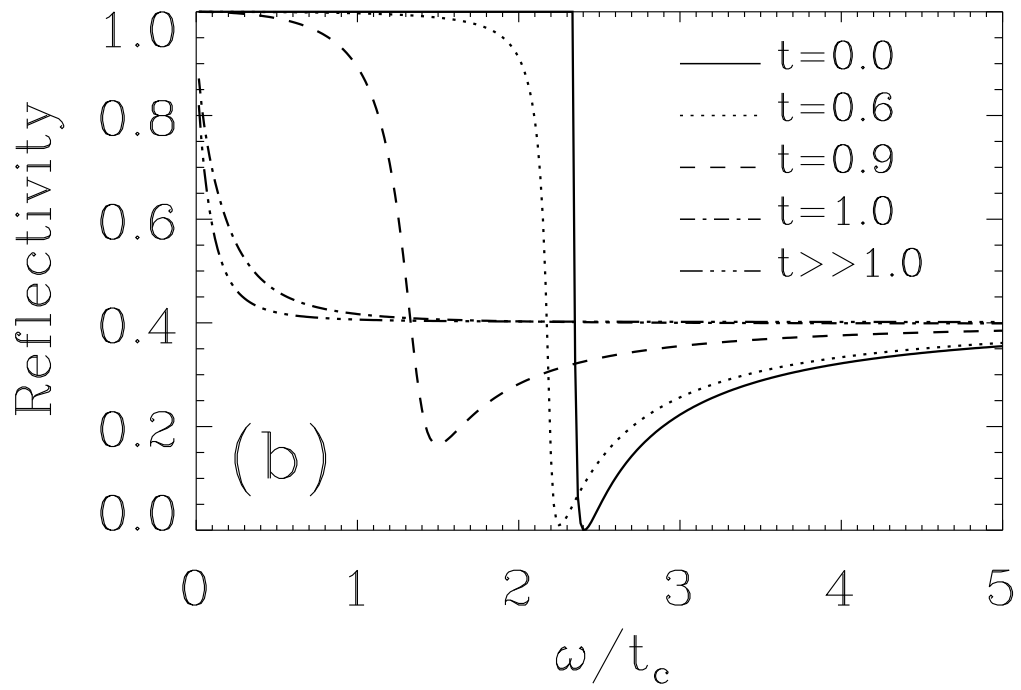
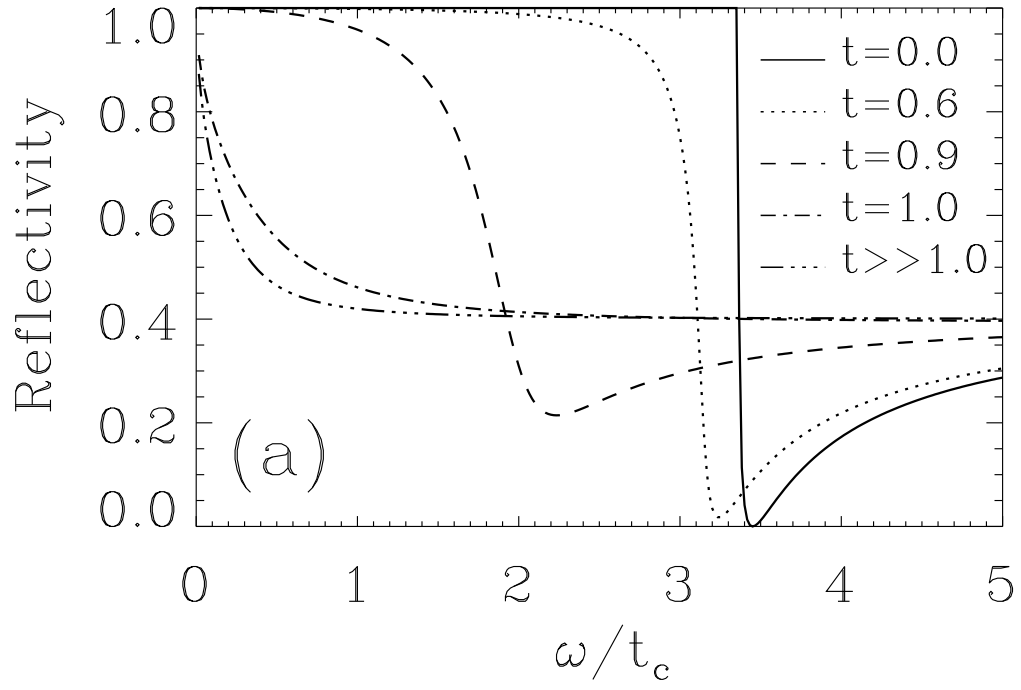
Sample	$\rho_c (T_c)$ m $\Omega$ -cm	$\rho_{ab} (T_c)$ $\mu\Omega$ -cm	$t_c$ cm $^{-1}$	$\gamma$ cm $^{-1}$	$\omega_{pl}$ (0 K) cm $^{-1}$	$\omega_{pl}$ (exp.) cm $^{-1}$
La <sub>1.84</sub> Sr <sub>0.16</sub> CuO <sub>4</sub>	50 [11]	140 [11]	23	330	57	55 [1]
Tl <sub>2</sub> Ba <sub>2</sub> CuO <sub>6</sub>	100 [12]	100 [12]	12	300	30	$\leq 30$ [13]
YBa <sub>2</sub> Cu <sub>3</sub> O <sub>6.6</sub>	200 [14]	100 [14]	9	570	55	60 [15]
Bi <sub>2</sub> Sr <sub>2</sub> CaCu <sub>2</sub> O <sub>8</sub>	10 <sup>4</sup> [16]	25 [16]	0.3	100	5	$\leq 7.5$ [17]



Das Sarma and Hwang, Fig. 1 (a),(b)



Das Sarma and Hwang, Fig. 1 (c)(d)



Das Sarma and Hwang, Fig. 2